Liquid Crystals
Publication details, including instructions for authors and subscription information:
http://www.informaworld.com/smpp/title~content=t713926090

Novel liquid crystal trimers exhibiting a monolayer smectic C phase containing strong macroscopic fluctuations

Atsushi Yoshizawa[a]; Naoki Uehara[a]; Mariko Kurauchi[a]; Akihisa Yamaguchi[a]
[a] Department of Frontier Materials Chemistry, Faculty of Science and Technology, Hirosaki University, Hirosaki 036-8561, Japan

To cite this Article Yoshizawa, Atsushi , Uehara, Naoki , Kurauchi, Mariko and Yamaguchi, Akihisa(2007) 'Novel liquid crystal trimers exhibiting a monolayer smectic C phase containing strong macroscopic fluctuations', Liquid Crystals, 34: 10, 1121 — 1128

To link to this Article: DOI: 10.1080/02678290701527560

URL: http://dx.doi.org/10.1080/02678290701527560

Liquid Crystals, Vol. 34, No. 10, October 2007, 1121–1128

Novel liquid crystal trimers exhibiting a monolayer smectic C phase containing strong macroscopic fluctuations

ATSUSHI YOSHIZAWA*, NAOKI UEHARA, MARIKO KURAUCHI and AKIHISA YAMAGUCHI

Department of Frontier Materials Chemistry, Faculty of Science and Technology, Hirosaki University, 3 Bunkyo-cho, Hirosaki 036-8561, Japan

(*Received 13 March 2007; accepted 2 June 2007*)

We prepared a homologous series of novel liquid crystal trimers, 1,4-bis(4-{ω-[4-(5-dodecylpyrimidine-2-yl)phenyloxy]alkyloxyphenyl}carbonyloxy)benzene, **I-(m, n)**, and investigated their physical properties using optical microscopy, differential scanning calorimetry and X-ray diffraction. All the compounds exhibited enantiotropic nematic (N) and smectic C (SmC) phases. Pronounced odd–even effects were apparent for the transition properties on varying the spacer length. X-ray diffraction measurements suggest that the SmC phase has a monolayer structure in which the molecular long axis is tilted to the layer normal. Furthermore, formation of defect-lines was observed for the SmC phases.

1. Introduction

Design of novel supermolecules is a promising approach to the production of liquid-crystalline phases that have a hierarchical structure. Supramolecular assemblies comprising supermolecules, i.e. dimeric and oligomeric liquid crystals, are a current topic in the field of liquid-crystalline chemistry [1]. Dimeric liquid crystals are attractive because they exhibit different properties from the corresponding low-molecular mass mesogens [2–5]. For instance, transition properties of dimeric liquid crystals are known to depend on the length and parity of the flexible spacer. Furthermore, liquid crystal trimers [6–15] and tetramers [16, 17] have been reported. Pronounced odd–even effects have been observed in the transition properties of linear liquid crystal oligomers on varying the spacer length. The transition behaviour is interpreted in terms of how the spacers control the average molecular shape [12, 16]. Recently, Imrie *et al.* reported non-symmetric trimers that exhibit a triply-intercalated alternating smectic C (SmC) phase [18, 19]. Goodby noted effects of oligomeric systems on appearance of the frustrated phases [20]. Monolayer organization vs. intercalation of the dimesogens can engender commensurate and/or incommensurate structuring. Competition between the two incommensurate lengths was found to induce formation of two-dimensional (2D) and/or incommensurate smectic phases. Coupling between chirality and oligomeric structure can produce novel phenomena. Nishiyama *et al.* reported a novel dichiral twin compound showing a broad temperature range of the smectic Q phase [21–23]. Introduction of a bent-shape molecular structure is another important strategy in the design of supermolecules. In the 1,3-benzene derivatives first synthesized by Akutagawa *et al.* [24], antiferroelectric and ferroelectric properties were described by Watanabe and co-workers [25, 26]. The rigid banana-shaped system has suggested new concepts for chirality and phase structures in liquid crystals [27–29]. Recently, Izumi *et al.* reported three types of dimeric smectic liquid cystals showing antiferroelectricity, frustration and chisality [30].

We have reported novel liquid crystal oligomers with a frustrated phase: a U-shaped molecule [31], a binaphthyl derivative [32, 33], a T-shaped compound [34] and a λ–shaped molecule [35]. We have investigated physical properties for a homologous series of bimesogenic liquid crystals, α-(4-cyanobiphenyl-4′-yloxy)-ω-[4-(5-alkylpyrimidine-2-yl)phenyl-4″-oxy]alkane (**mPYnOCB**) [36, 37], and recently reported the observation of a striped pattern in the interdigitated anticlinic SmC phase of a homeotropically aligned sample of binary mixtures between the bimesogenic compounds [38].

In this paper, we report the design of a novel liquid crystal trimer in which two bimesogenic compounds are incorporated in a single molecule. The design concept is shown in figure 1. We prepared a homologous series of novel liquid crystal trimers, 1,4-bis(4-[ω-{4-(5-dodecyl-pyrimidine-2-yl)phenyloxy}alkyloxyphenyl]carbonyloxy) benzene, **I-(m, n)**, and investigated the effects of the parity of the spacers on their transition behaviour and phase structure.

---

*Corresponding author. Email: ayoshiza@cc.hirosaki-u.ac.jp

Liquid Crystals
ISSN 0267-8292 print/ISSN 1366-5855 online © 2007 Taylor & Francis
http://www.tandf.co.uk/journals
DOI: 10.1080/02678290701527560

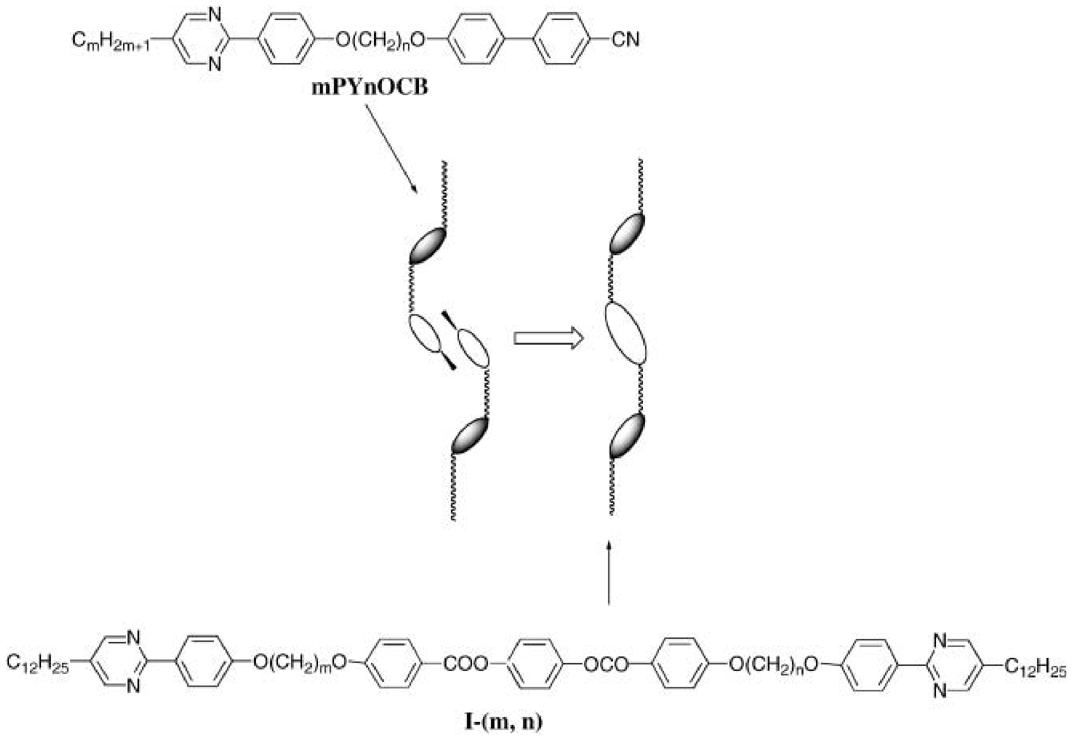

Figure 1. Design concept of the novel liquid crystal trimer.

2. Experimental

2.1. *Preparation of materials*

5-Dodecyl-2-(4-hydroxyphenyl)pyrimidine was obtained from Midori Kagaku Co., Ltd. The liquid crystal oligomer **I-(7, 7)** was prepared according to the synthesis process outlined in scheme 1.

Purification of final products was carried out using column chromatography over silica gel (63–210 μm) (Kanto Chemical Co, Inc) using dichloromethane or a dichloromethane–ethyl acetate mixture as the eluent, followed by recrystallization from ethanol. The purities of final compounds were checked by thin-layer chromatography (TLC, aluminum sheets, silica gel 60 F254 from Merck). Dichloromethane was used as the solvent. Detection of products was achieved by UV irradiation (λ=254 and 365 nm). The purity of the final compound was checked by HPLC (Japan Analytical Industry Co, Ltd, LC9101, JAIGEL-1H column). Chloroform was used as eluent. Detection of products was achieved by UV irradiation (λ=254 nm).

The structures of the final products were elucidated by IR spectroscopy (FTS-30; BIO RAD) and ^{1}H NMR spectroscopy (JNM-A400, JEOL or JNM-ECA500, JEOL).

2.1.1. 1,4-Bis(4-{7-[4-(5-dodecylpyrimidine-2-yl) phenyloxy]heptyloxyphenyl}carbonyloxy)benzene, I-(7, 7).

Potassium carbonate (0.35 g, 0.25 mmol) was added to a solution of 1,7-dibromoheptane (0.96 g, 3.8 mmol) and 5-dodecyl-2-(4-hydroxyphenyl)pyrimidine (0.85 g, 2.5 mmol) in cyclohexanone (10 ml). The reaction mixture was stirred at 80°C for 6 h. After filtration of the precipitate, the solvent was removed by evaporation. The residue was purified by column chromatography on silica gel with dichloromethane. Recrystallization from hexane gave 5-dodecyl-2-{4-(7-bromoheptyloxy)}pyrimidine; yield 0.62 g (48%).

Potassium carbonate (0.17 g, 1.2 mmol) and potassium iodide (0.03 g, 1.8 mmol) were added to a solution of ethyl 4-hydroxybenzoate (0.20 g, 1.2 mmol) and 5-dodecyl-2-{4-(7-bromoheptyloxy)}pyrimidine (0.62 g, 1.2 mmol) in cyclohexanone (10 ml). The reaction mixture was stirred at 80°C for 3 h. After filtration of the precipitate, the solvent was removed by evaporation. The residue was purified by column chromatography on silica gel with dichloromethane. Recrystallization from ethanol gave ethyl 4-{7-[4-(5-dodecylpyrimidine-2-yl)phenyloxy]heptyloxy}benzoate; yield 0.41 g (57%).

Ethyl 4-{7-[4-(5-dodecylpyrimidine-2-yl)phenyloxy]-heptyloxy}benzoate (0.39 g, 0.65 mmol) was added to a solution of 85% KOH (0.18 g, 2.7 mmol) in an ethanol–water (19:1) mixture. The resulting solution was stirred at 90°C for 2 h. The solution was acidified with aq. HCl. The solution was extracted with

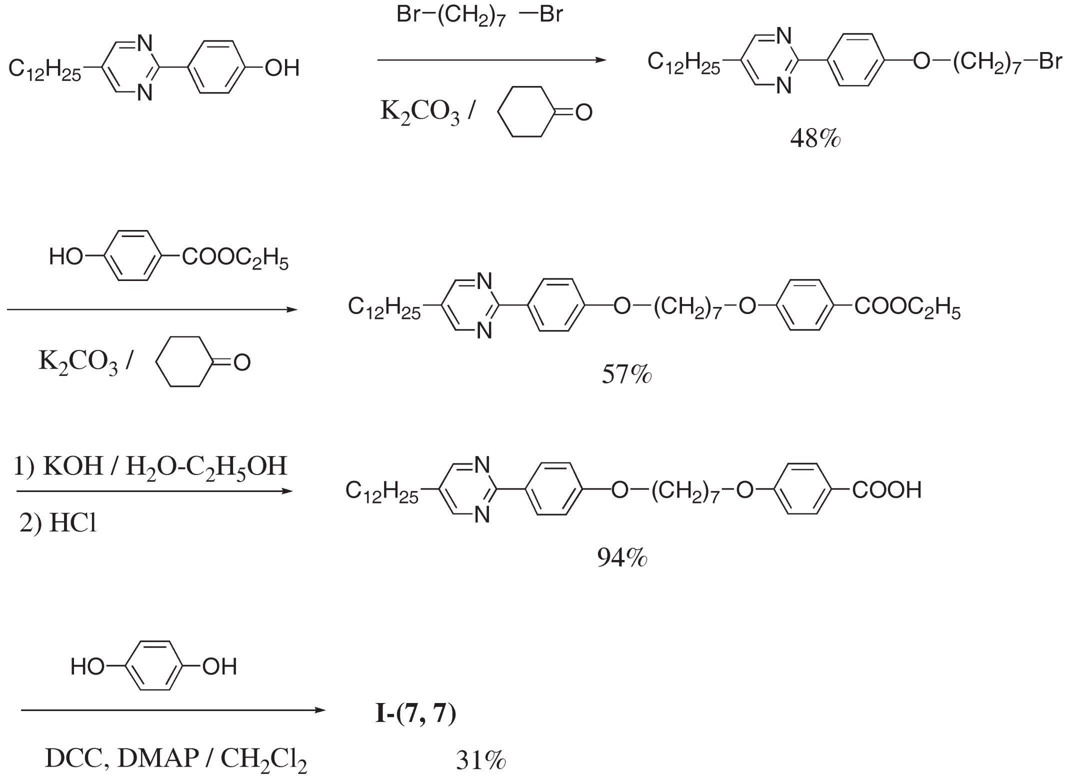

Scheme 1. Synthesis of **I-(7, 7)**.

dichloromethane. The organic layers were combined, dried over sodium sulfate, filtered and evaporated. 4-{7-[4-(5-Dodecylpyrimidine-2-yl)phenyloxy]heptyloxy}benzoic acid was obtained; yield 0.35 g (94%).

To a solution of 4-{7-[4-(5-dodecylpyrimidine-2-yl)phenyloxy]heptyloxy}benzoic acid (0.33 g, 0.57 mmol) in dichloromethane (25 ml), 1,4-dihydroxybenzene (0.03 g, 0.27 mmol), *N*,*N*′-dicyclohexylcarbodiimide (0.18 g, 0.87 mmol) and 4-(*N*,*N*-dimethylamino)pyridine (0.02 g, 0.16 mmol) were added. The resulting solution was stirred at room temperature overnight. Precipitated materials were removed by filtration. After removal of the solvent by evaporation, the residue was purified by column chromatography on silica gel with a dichloromethane–ethyl acetate (30:1) mixture as the eluent. Recrystallization from ethanol gave the desired product; yield 0.11 g (31%). ^{1}H NMR (400 MHz, solvent $CDCl_3$, standard TMS) δ_H/ppm: 8.57 (s, 4H, Ar–**H**), 8.35 (d, 4H, Ar–**H**, J=8.8 Hz), 8.14 (d, 4H, Ar–**H**, J=8.8 Hz), 7.26 (s, 4H, Ar–**H**), 6.98 (d, 4H, Ar–**H**, J=9.1 Hz), 6.98(d, 4H, Ar–**H**, J=8.8 Hz), 4.06 (t, 4H, –OC**H**$_2$, J=5.8 Hz), 4.05 (t, 4H, –OC**H**$_2$, J=5.8 Hz), 2.59 (t, 4H, Ar–C**H**$_2$–, J=7.6 Hz), 1.85–1.26 (m, 60H, aliphatic), 0.88 (t, 6H, –C**H**$_3$, J=6.8 Hz). IR (KBr) ν_{max}/cm^{-1}: 2927, 2849, 1734, 1606, 1582. Purity: 99.9%.

2.1.2. 1,4-Bis(4-{8-[4-(5-dodecylpyrimidine-2-yl)phenyloxy]octyloxyphenyl}carbonyloxy)benzene, I-(8, 8). ^{1}H NMR (400 MHz, solvent $CDCl_3$, standard TMS) δ_H/ppm: 8.57 (s, 4H, Ar–**H**), 8.34 (d, 4H, Ar–**H**, J=8.8 Hz), 8.14 (d, 4H, Ar–**H**, J=8.8 Hz), 7.26 (s, 4H, Ar–**H**), 6.98 (d, 4H, Ar–**H**, J=8.9 Hz), 6.97 (d, 4H, Ar–**H**, J=8.8 Hz), 4.05 (t, 4H, –OC**H**$_2$, J=5.7 Hz), 4.04 (t, 4H, –OC**H**$_2$, J=5.8 Hz), 2.59 (t, 4H, Ar–C**H**$_2$–, J=7.6 Hz), 1.83–1.26 (m, 64H, aliphatic), 0.88 (t, 6H, –C**H**$_3$, J=6.7 Hz). IR (KBr) ν_{max}/cm^{-1}: 2924, 2852, 1718, 1606, 1583. Purity: 100%.

2.1.3. 1,4-Bis(4-{9-[4-(5-dodecylpyrimidine-2-yl)phenyloxy]nonyloxyphenyl}carbonyloxy)benzene, I-(9, 9). ^{1}H NMR (400 MHz, solvent $CDCl_3$, standard TMS) δ_H/ppm: 8.55 (s, 4H, Ar–**H**), 8.32 (d, 4H, Ar–**H**, J=8.8 Hz), 8.12 (d, 4H, Ar–**H**, J=8.9 Hz), 7.24 (s, 4H, Ar–**H**), 6.96 (d, 4H, Ar–**H**, J=9.0 Hz), 6.95 (d, 4H, Ar–**H**, J=8.8 Hz), 4.03 (t, 4H, –OC**H**$_2$, J=5.9 Hz), 4.01 (t, 4H, –OC**H**$_2$, J=5.9 Hz), 2.57 (t, 4H, Ar–C**H**$_2$–, J=7.7 Hz), 1.83–1.23 (m, 68H, aliphatic), 0.86 (t, 6H, –C**H**$_3$, J=6.8 Hz). IR (KBr) ν_{max}/cm^{-1}: 2920, 2850, 1734, 1605, 1582. Purity: 100%.

2.1.4. 1-(4-{7-[4-(5-Dodecylpyrimidine-2-yl)phenyloxy]heptyloxyphenyl}carbonyloxy)-4-(4-{8-[4-(5-dodecylpyrimidine-2-yl)phenyloxy]octyloxyphenyl}carbonyloxy)benzene, I-(7, 8). To a solution of 4-{8-[4-(5-dodecylpyrimidine-2-yl) phenyloxy]octyloxy}benzoic acid (0.38 g, 0.65 mmol) in dichloromethane (30 ml), 1,4-dihydroxybenzene (0.14 g, 1.3 mmol), *N*,*N*′-dicyclohexylcarbodiimide (0.21 g, 1.0 mmol) and 4-(*N*,*N*-dimethylamino)pyridine (0.01 g, 0.10 mmol) were added. The resulting solution was stirred at room temperature overnight. Precipitated materials were removed by filtration. After removal of the solvent by evaporation, the residue was purified by column chromatography on silica gel with a dichloromethane–ethyl acetate (30:1) mixture as the eluent. 1-(4-{8-[4-(5-dodecylpyrimidine-2-yl)phenyloxy] octyloxyphenyl}carbonyloxy)-4-hydroxybenzene was obtained; yield 0.07 g (10%).

To a solution of 4-{7-[4-(5-dodecylpyrimidine-2-yl)phenyloxy]heptloxy}benzoic acid (0.07 g, 1.22 mmol) and 1-(4-{8-[4-(5-dodecylpyrimidine-2-yl)phenyloxy]octyloxyphenyl}carbonyloxy)-4-hydroxybenzene (0.07 g, 1.05 mmol) in dichloromethane (30 ml), *N*,*N*′-dicyclohexylcarbodiimide (0.49 g, 2.38 mmol) in dichloromethane and 4-(*N*,*N*-dimethylamino)pyridine (0.04 g, 0.33 mmol) were added. The resulting solution was stirred at room temperature overnight. Precipitated materials were removed by filtration. After removal of the solvent by evaporation, the residue was purified by column chromatography on silica gel with a dichloromethane–ethyl acetate (30:1) mixture as the eluent and then purified using HPLC with chloroform. Reprecipitation with dichloromethane/toluene gave the target compound; yield 0.04 g (31%). ^{1}H NMR (400 MHz, solvent $CDCl_3$, standard TMS) δ_H/ppm: 8.57 (s, 4H, Ar–**H**), 8.35 (d, 4H, Ar–**H**, J=8.8 Hz), 8.14 (d, 4H, Ar–**H**, J=8.8 Hz), 7.26 (s, 4H, Ar–**H**), 6.98 (d, 4H, Ar–**H**, J=8.8 Hz), 6.97 (d, 4H, Ar–**H**, J=8.8 Hz), 4.06–4.02 (m, 8H, –O$\mathbf{CH_2}$), 2.59 (t, 4H, Ar–$\mathbf{CH_2}$–, J=7.6 Hz), 1.84–1.26 (m, 62H, aliphatic), 0.88 (t, 6H, –$\mathbf{CH_3}$, J=6.8 Hz). IR (KBr) ν_{max}/cm^{-1}: 2921, 2849, 1733, 1606, 1582. Purity: 100 %.

2.1.5. 1-(4-{7-[4-(5-dodecylpyrimidine-2-yl)phenyloxy] heptyloxyphenyl}carbonyloxy)-4-(4-{8-[4-(5-dodecylpyrimidine-2-yl)phenyloxy]nonyloxyphenyl}carbonyloxy)benzene, I-(7, 9).

^{1}H NMR (500 MHz, solvent $CDCl_3$, standard TMS) δ_H/ppm: 8.55 (s, 4H, Ar–**H**), 8.32 (d, 4H, Ar–**H**, J=8.8 Hz), 8.14 (d, 4H, Ar–**H**, J=8.8 Hz), 7.25 (s, 4H, Ar–**H**), 6.98 (d, 4H, Ar–**H**, J=8.1 Hz), 6.98 (d, 4H, Ar–**H**, J=8.8 Hz), 4.06 (t, 2H, –O$\mathbf{CH_2}$, J=6.3 Hz), 4.05 (t, 4H, –O$\mathbf{CH_2}$, J=6.3 Hz), 4.03 (t, 2H, –O$\mathbf{CH_2}$, J=6.4 Hz), 2.59 (t, 4H, Ar–$\mathbf{CH_2}$–, J=7.6 Hz), 1.85–1.26 (m, 64H, aliphatic), 0.88 (t, 6H, –$\mathbf{CH_3}$, J=7.0 Hz). IR (KBr) ν_{max}/cm^{-1}: 2922, 2851, 1732, 1606, 1583. Purity: 99.9%.

2.2. *Liquid-crystalline and physical properties*

The initial phase assignments and corresponding transition temperatures for the final products were determined using thermal optical microscopy with a polarizing microscope (Optiphoto POL; Nikon Corp) equipped with a Mettler FP82 microfurnace and FP80 control unit. The heating and cooling rates were 5°C min^{-1}. Temperatures and enthalpies of transition were investigated using differential scanning calorimetry (DSC) using a Seiko DSC 6200 calorimeter. The materials were studied at a scanning rate of 5°C min^{-1}, for both heating and cooling cycles, after being encapsulated in aluminum pans. X-ray scattering experiments were performed using an X-ray diffractometer (Rigaku RU-200) or a real time X-ray diffractometer (Bruker AXS D8 Discover). The textural changes, as a function of applied ac electric field, were investigated for a sample contained in a homogeneous configuration cell (5 μm) where the inner surfaces had been coated with a polyimide aligning agent and unidirectionally buffered.

3. Results and discussion

3.1. *Physical properties*

The transition temperatures and associated entropy changes, $\Delta S/R$, for **I-(m, n)** are listed in table 1.

All the compounds exhibited enantiotropic nematic (N) and SmC phases. **I-(8, 8)**, **I-(9, 9)**, **I-(7, 8)** and **I-(7, 9)** exhibited a smectic I (SmI) phase below their SmC phase. Pronounced odd–even effects are seen for the isotropic (I)–N and N–SmC transition temperatures of the symmetric trimers as the parity of the spacers is varied. The even-membered trimers exhibit higher values. Although precise entropy changes at the I–N and N–SmC transitions of **I-(8, 8)** were unobtainable

Table 1. Transition temperatures (°C) and $\Delta S/R$ (in parentheses) for **I-(m, n)**. Square brackets indicate a monotropic transition.

	Cr	SmI	SmC	N	I
I-(7, 7)	• 142 (22)		• 171 (1.0)	• 180 (0.9)	•
I-(8, 8)	• 135 (18)	• 139 (1.1)	• 196[a]	• 198[a]	•
I-(9, 9)	• 128 (35)	[• 121 (2.4)]	• 158 (0.8)	• 172 (1.2)	•
I-(7, 8)	• 131 (18)	[• 125 (0.8)]	• 184 (0.8)	• 189 (1.5)	•
I-(7, 9)	• 122 (20)	• 123 (2.0)	• 164 (1.4)	• 176 (1.3)	•

[a] The I–N and N–SmC transitions occurred simultaneously.

because of the partial overlap of the two transition peaks, their values are estimated, respectively, as 5.2 and 2.5. Therefore, we can say that the entropy changes at those transitions show marked odd–even effects.

Figure 2 shows the textures of a sample of **I-(7, 7)** on a glass plate with a cover glass. The broken fan texture in the planar aligned region (figure 2 a) and schlieren texture in the homeotropic aligned region (figure 2 b) are apparent. They are characteristic textures of the SmC phase. The schlieren texture possesses a point singularity with four (s=1/4) brushes only, indicating that the SmC phase has a synclinic structure. In investigations of the SmC textures exhibited by **I-(7, 7)** we observed intense and extensive fluctuation, i.e. incessant change of birefringence in a small domain, in boundary regions between the planarly aligned and homeotropically aligned regions as the temperature was changed.

Layer spacing in the SmC phase of 54.4 Å was obtained from X-ray diffraction measurements for **I-(7, 7)** at 160°C. This did not change with decreasing temperature in the SmC phase. The molecular length was estimated from MM2 models to be about 79 Å. The layer spacing is shorter than the molecular length, but longer than layer spacings in the possible intercalated structures. Therefore, the SmC phase is inferred to have a monolayer structure in which the molecular long axes are tilted to the layer normal.

The trimer **I-(8, 8)** with even-membered spacers exhibited enantiotropic N, SmC and SmI phases. Textures of the SmC phase resembled those of **I-(7, 7)** with odd-membered spacers. Strong fluctuation of the SmC texture was also observed for **I-(8, 8)**. The N and SmC phases of both **I-(7, 7)** and **I-(8, 8)** proved to be miscible across the full composition range, indicating that the SmC phase of **I-(8, 8)** has the same long-range order as that of **I-(7, 7)**. The SmI phase was identified by optical microscopy. On cooling the schlieren texture of the preceding SmC phase, the resulting texture was of a schlieren form, which was difficult to bring into microscopic focus, as shown in figure 3. This texture observation is characteristic of a transition from SmC to SmI.

The trimer **I-(9, 9)** with odd-membered spacers exhibited enantiotropic N and SmC phases, and exhibited a monotropic SmI phase. Fluctuation was observed in the SmC phase not only with changing temperature, but also at constant temperature. Furthermore, the SmC phase partly showed defect lines that were similar to the chiral SmC phase, as depicted in figure 4. The defect lines were also observed in the SmC phases of **I-(8, 8)**, **I-(7, 8)** and **I-(7, 9)**, whereas they were not observed in the SmC phases of **I-(7, 7)**. Below the SmC phase of **I-(9, 9)**, a monotropic SmI phase appeared.

Figure 5 shows X-ray diffraction patterns in the small-angle region for **I-(9, 9)** in the SmC and SmI phases. In the SmC phase at 140°C, a sharp reflection, 2θ=1.49°, was observed in the small-angle region, corresponding to a spacing of 59.2 Å. Then, a shaper and stronger reflection at 2θ=1.38° corresponding to a spacing of 63.9 Å was observed in the SmI phase at 110°C and the second reflection at 2θ=2.71° could be detected. Figure 6 shows temperature dependence of the layer spacings in the SmC and SmI phases. The layer spacing in the SmC phase is independent of temperature except in the vicinity of the SmC–SmI transition. The

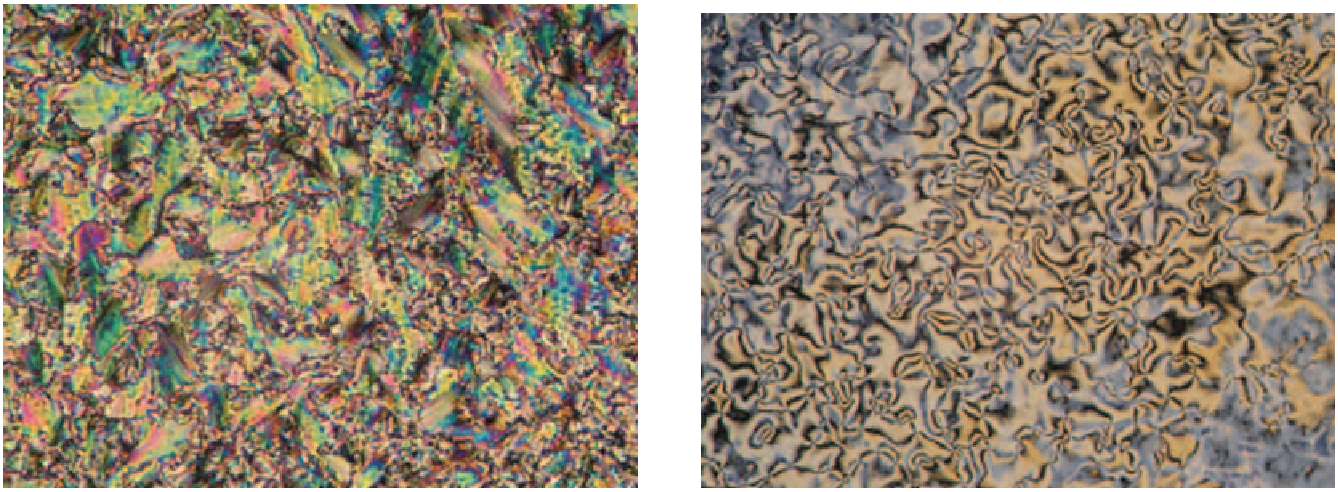
(*a*) (*b*)

Figure 2. Smectic C textures of **I-(7, 7)** on a glass slide with a cover glass showing the (a) fan texture in the planar aligned region at 169°C and (b) schlieren texture in the homeotropic aligned region at 165°C. Magnification 200×.

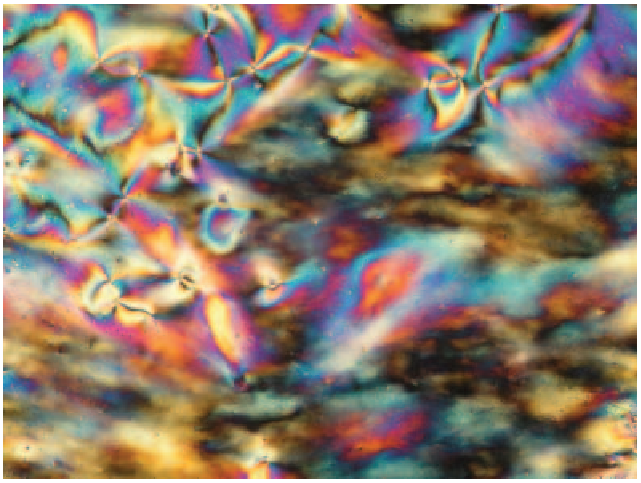

Figure 3. Texture of SmI phase of **I-(8, 8)** on a glass slide with a cover glass at 125°C. Magnification 200 ×.

layer spacing in the SmI phase was found to be longer than that in the SmC phase.

Trimer **I-(7, 8)**, which possesses both odd-membered and even-membered spacers, exhibited enantiotropic N and SmC phases, and a monotropic SmI phase. The I–N and N–SmC temperatures of **I-(7, 8)** are higher than those of **I-(7, 7)**, but lower than those of **I-(8, 8)**. Trimer **I-(7, 9)**, which possesses different odd-numbered spacers, exhibited enantiotropic N, SmC and SmI phases. The I–N and N–SmC temperatures of **I-(7, 9)** are higher than those of **I-(7, 7)**, but lower than those of **I-(9, 9)**.

A preliminary electro-optical study was performed for **I-(8, 8)**. Unusual textural changes, like a convective pattern, were observed in the SmC phase of a sample contained in an evaluation cell (5 μm) by applying an ac field of ±12 V μm^{-1} in the frequency range from 1 Hz to 100 Hz. The changes were different from ferroelectric and antiferroelectric switching behaviour. Further investigations are in progress.

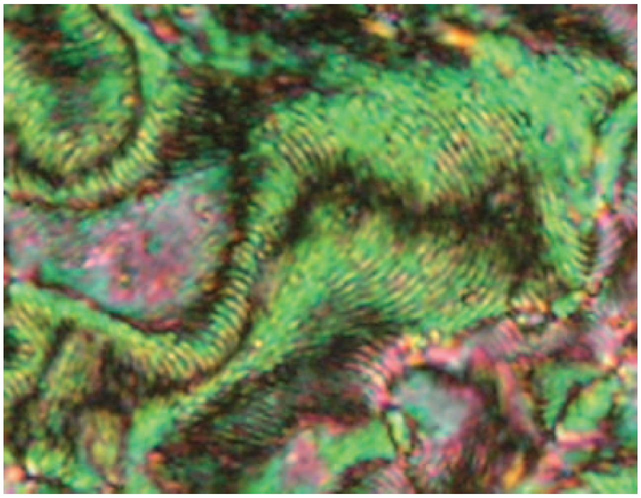

Figure 4. Lines in the SmC phase of **I-(9, 9)** on a glass slide with a cover glass at 149°C. Magnification 200 ×.

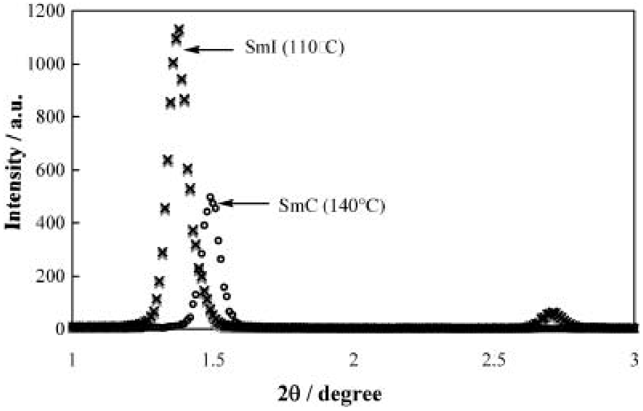

Figure 5. X-ray diffraction pattern of **I-(9, 9)** in the SmC (140°C) and SmI (110°C) phases.

3.2. *Molecular organization*

The trimers **I-(7, 7)** and **I-(9, 9)** were found to form a monolayer SmC phase by XRD measurements. Imrie *et al.* reported non-symmetric liquid crystal trimers with a triply-intercalated alternating smectic phase [18, 19]. They noted that the driving force for smectic formation is a combination of molecular shape and a specific interaction between unlike mesogenic units. Long terminal chains of the present trimer **I-(m, n)** are thought to prohibit the trimer from forming an intercalated structure. The marked odd–even effects for the transition properties of all trimers suggest that the trimers exist in their extended conformations in their N and SmC phases. The assumption that the trimers exist only in their extended conformations is insufficient

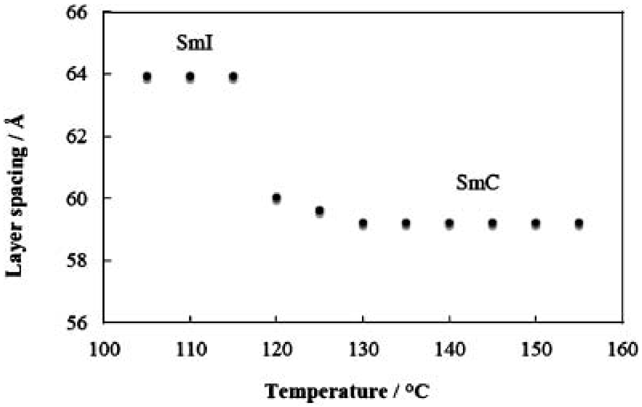

Figure 6. Temperature dependence of the layer spacing of **I-(9, 9)** in the SmC and SmI phases.

to discuss their structure–property relationships. Imrie and Luckhurst give the following interpretation for odd–even effects for transition properties of dimesogenic compounds [2a, 12, 14]. In the isotropic phase, approximately half the conformers of an even-membered dimer are essentially linear, whereas for an odd-membered dimer, only 10% are linear. There exists a synergy between conformation and orientational order. Therefore, at the transition to the nematic phase for even-membered dimers, many of the bent conformers are converted to a linear form. This enhances the orientational order of the nematic phase, engendering a larger nematic–isotropic entropy than would be expected for a monomer. For odd-membered dimers, however, the difference in free energy between the bent and linear conformers is such that the orientational order of the nematic phase is insufficient to convert bent into linear conformers. Consequently, the orientational order is not enhanced and smaller nematic–isotropic entropy is expected. Based on the assumption that this treatment is applicable for transition properties of the present trimers, the marked odd–even effects in the I–N transition properties of the trimers lead us to assume an extended conformation for the trimers in their N phases. Figure 7 shows schematic sketches for the trimers with all-trans conformations of the spacers. Trimers with odd-membered spacers, **I-(7, 7)**, **I-(9, 9)** and **I-(7, 9)**, have a zigzag shape in which all three mesogenic units are inclined with respect to each other, whereas a trimer with even-membered spacers **I-(8, 8)** has a linear shape in which the three mesogenic units are coparallel. A trimer with odd-membered and even membered spacers **I-(7, 8)** has a hockey-stick-like shape, in which two mesogenic units are coparallel, whereas the third is inclined to the other two.

Next, we examine the structures of SmC phases formed by the trimers. Pronounced odd–even effects are also seen for the N–SmC transition temperatures of the trimers. These results indicate that same argument as for the I–N transition is applicable for the N–SmC transition. Efficient molecular packing requires the smallest excluded volume for a molecule in a layer structure. The molecular long axis is tilted with respect to the layer normal. The conformation in the SmC phase is thought to be a zigzag structure, as in the N phase (see figure 7 a), which engenders the small entropy change at the N–SmC transition. The SmC phase has a synclinc structure in which the zigzag structure might coexist in each layer. If this is the case, the SmC phase might have three directors: an *n*-director, which represents an orientational vector of the long axis; *c*-director, which represents the tilt direction of the long axis; and the third director, which represents an orientational vector of the short axis. The acronym referring to the third director is the *m*-director in this paper. Different patterns of molecular packing exist in each layer, which produces a distribution of the *m*-director. Exchange among the different molecular packing patterns can occur easily by changing the temperature, which can cause intense fluctuation in boundary regions between the planarly aligned and homeotropically aligned regions.

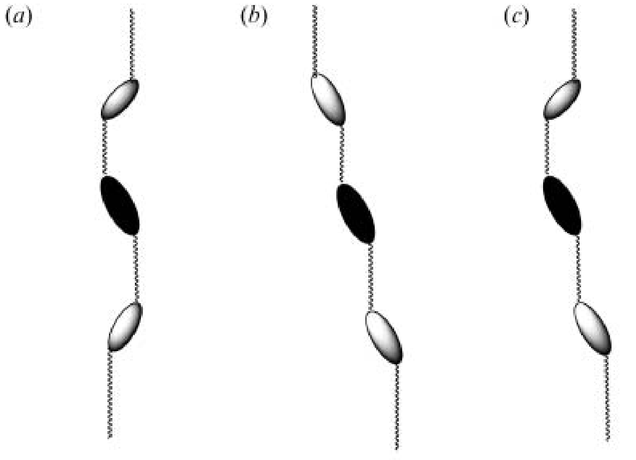

I-(7, 7), I-(9, 9), I-(7, 9) **I-(8, 8)** **I-(7, 8)**

Figure 7. Schematic sketches for the trimers.

4. Conclusion

A homologous series of novel liquid crystal trimers, 1,4-bis(4-{ω-[4-(5-dodecylpyrimidine-2-yl)phenyloxy]alkyloxyphenyl}carbonyloxy)benzene, **I-(m, n)**, has been prepared. The trimers exhibited enantiotropic N and SmC phases, and strong fluctuation was observed in their SmC phases when changing their temperature. XRD measurements indicate that the SmC phases of trimers **I-(7, 7)** and **I-(9, 9)** have a monolayer structure in which the three mesogenic units are tilted to each other. Macroscopic fluctuations that are observed in the SmC phases can be interpreted in terms of exchange among the different molecular packing patterns within the layers. Furthermore, the trimers which have a SmI phase were found to induce defect lines in the SmC phase.

Acknowledgements

We thank Prof. Y. Maeda for X-ray measurements of **I-(7, 7)** and also thank Prof. J. Yamamoto for X-ray measurements of **I-(9, 9)**. This work was partly supported by Aomori Prefecture Collaboration of Regional Entities for the Advancement of Technological Excellence, JST and a Grant for

Priority Research Designated by the President of Hirosaki University.

References

[1] (a) J.W. Goodby, G.H. Mehl, I.M. Saez, R.P. Tuffin, G. Mackenzie, R. Auzely-Velty, T. Benvegnu, D. Plusquellec. *Chem. Commun.* 2057 (1998); (b) I. Saez, J.W. Goodby. *J. Mater. Chem.*, **15**, 26 (2005).

[2] (a) C.T. Imrie, G.R. Luckhurst. In *Handbook of Liquid Crystals* Vol. 1, D. Demus, J.W. Goodby, G.W. Gray, H.W. Spiess, V. Vill (Eds), pp. 801–833, Wiley-VCH, Weinheim (1998), (b) C.T. Imrie, *Struct. Bond.*, **96**, 149 (1999); (c) C.T. Imrie, P.A. Henderson. *Curr. Opinions Colloid Interface Sci.*, **7**, 298 (2002).

[3] J.W. Emsley, G.R. Luckhurst, G.N. Shilstone, I. Sage. *Mol. Cryst. liq. Cryst.*, **102**, 223 (1984).

[4] A.C. Griffin, T.R. Britt. *J. Am. chem. Soc.*, **103**, 4957 (1981).

[5] R.W. Date, C.T. Imrie, G.R. Luckhurst, J.M. Seddon. *Liq. Cryst.*, **12**, 203 (1992).

[6] P. Keller. *Mol. Cryst. liq. Cryst.*, **123**, 247 (1985).

[7] H. Furuya, K. Asahi, A. Abe. *Polymer J.*, **18**, 779 (1986).

[8] G.S. Attard, C.T. Imrie. *Liq. Cryst.*, **6**, 387 (1989).

[9] R. Centore, A. Roviello, A. Sirigu. *Mol. Cryst. liq. Cryst.*, **182B**, 233 (1990).

[10] T. Ikeda, T. Miyamoto, S. Kurihara, M. Tsukada, S. Tazuke. *Mol. Cryst. liq. Cryst.*, **182B**, 357 (1990).

[11] N.V. Tsvetkov, V.V. Zuev, V.N. Tsvetkov. *Liq. Cryst.*, **22**, 245 (1997).

[12] C.T. Imrie, G.R. Luckhurst. *J. Mater. Chem.*, **8**, 1339 (1998).

[13] G.R. Luckhurst. *Macromol. Symp.*, **96**, 1 (1995).

[14] B.-Q. Chen, A. Kameyama, T. Nishikubo. *Macromolecules*, **32**, 6485 (1999).

[15] P.A. Henderson, A.G. Cook, C.T. Imrie. *Liq, Cryst.*, **31**, 1427 (2004).

[16] C.T. Imrie, D. Stewart, C. Remy, D.W. Christie, I.W. Hamley, R. Harding. *J. Mater. Chem.*, **9**, 2321 (1999).

[17] P.A. Henderson, C.T. Imrie. *Liq. Cryst.*, **32**, 1531 (2005).

[18] C.T. Imrie, P.A. Henderson, J.M. Seddon. *J. Mater. Chem.*, **14**, 2486 (2004).

[19] P.A. Henderson, C.T. Imrie. *Liq. Cryst.*, **32**, 673 (2005).

[20] J.W. Goodby. *Curr. Opinions Colloid Interface Sci.*, **7**, 326 (2002).

[21] I. Nishiyama, J. Yamamoto, J.W. Goodby, H. Yokoyama. *Proc. SPIE*, **5518**, 201 (2004).

[22] I. Nishiyama, J. Yamamoto, J.W. Goodby, H. Yokoyama. *J. Mater. Chem.*, **11**, 2690 (2001).

[23] I. Nishiyama, J. Yamamoto, J.W. Goodby, H. Yokoyama. *J. Mater. Chem.*, **12**, 1709 (2002).

[24] T. Akutagawa, Y. Matsunaga, K. Yasuhara. *Liq. Cryst.*, **17**, 659 (1994).

[25] T. Niori, T. Sekine, J. Watanabe, T. Furukawa, H. Takezoe. *J. Mater. Chem.*, **6**, 1231 (1996).

[26] E. Grecka, D. Pociecha, F. Araoka, D.R. Link, M. Nakata, J. Thisayukta, Y. Takanishi, K. Ishikawa, J. Watanabe, H. Takezoe. *Phys. Rev. E*, **62**, R4524 (2000).

[27] D.R. Link, G. Natale, R. Shao, J.E. Maclennan, N.A. Clark, E. Korblova, D.M. Walba. *Science*, **278**, 1924 (1997).

[28] G. Pelzl, S. Diele, W. Weissflog. *Adv. Mater.*, **11**, 707 (1999).

[29] H. Takezoe, Y. Takanishi. *Jap. J. appl. Phys., Pt. 1*, **45**, 597 (2006).

[30] T. Izumi, S. Kang, T. Niori, Y. Takanishi, H. Takezoe, J. Watanabe. *Jap. J. appl. Phys., Pt. 1*, **45**, 1506 (2006).

[31] A. Yoshizawa, A. Yamaguchi. *Chem. Commun.*, 2060 (2002).

[32] J. Rokunohe, A. Yoshizawa. *J. Mater. Chem.*, **15**, 275 (2005).

[33] J. Rokunohe, A. Yamaguchi, A. Yoshizawa. *Liq. Cryst.*, **32**, 207 (2005).

[34] A. Yoshizawa, M. Sato, J. Rokunohe. *J. Mater. Chem.*, **15**, 3285 (2005).

[35] A. Yamaguchi, I. Nishiyama, J. Yamamoto, H. Yokoyama, A. Yoshizawa. *J. Mater. Chem.*, **15**, 280 (2005).

[36] A. Yoshizawa, N. Ise, T. Okada. *Ferroelectrics*, **214**, 75 (1998).

[37] A. Yoshizawa, K. Yamamoto, H. Dewa, I. Nishiyama, J. Yamamoto, H. Yokoyama. *J. Mater. Chem.*, **13**, 172 (2003).

[38] A. Yoshizawa, M. Kurauchi, Y. Kohama, H. Dewa, K. Yamamoto, I. Nishiyama, T. Yamamoto, J. Yamamoto, H. Yokoyama. *Liq. Cryst.*, **33**, 611 (2006).